



# Ternary copper(II) complexes with 1,10-phenanthroline and various aminoacidates: A spectroscopic and voltammetric study in aqueous solution

Gabriele Valora<sup>a</sup>, Gabriella Munzi<sup>b</sup>, Raffaele P. Bonomo<sup>a,\*</sup>

<sup>a</sup> Dipartimento di Scienze Chimiche, Università degli Studi di Catania, Viale A. Doria 6, 95125 Catania, Italy

<sup>b</sup> Consiglio nazionale delle Ricerche, Istituto di Microelettronica e Microsistemi, Via S. Sofia 64, 95123 Catania, Italy

## ABSTRACT

Ternary copper(II) complexes with 1,10-phenanthroline and the aminoacids L-arginine, L-aspartic acid, L-histidine, L-glutamic acid, L-glutamine, L-leucine, L-lysine, L-methionine, L-phenylalanine, L-tryptophan, L-tyrosine, L-valine, were studied in aqueous solution by means of UV–Vis–NIR spectrophotometry, EPR spectroscopy either at room or at low temperatures, and Square Wave Voltammetry. From the experimental data it is possible to conclude that most of these ternary complexes show a pseudo-octahedral geometry with a  $\text{CuN}_3\text{O}$  in plane chromophore and two oxygen atoms coming from water molecules perpendicularly bound to the equatorial plane. An exception to this general behaviour is given by the ternary copper(II) complex with 1,10-phenanthroline and histidine at pH value near the neutrality because of the terdentate nature of histidine when it coordinates by means of its histamine-like mode. In this case, evidence for a probable square-based pyramidal stereochemistry is given in support. At pH values around 5 the histidine behaves as bidentate ligand coordinating by its glycine-like mode, so as the copper (II) ternary complex with 1,10-phenanthroline shows the pseudo-octahedral geometry found for all the ternary complexes with the other aminoacids. Moreover the ternary complex species with histidine at pH 5 and 7 are in equilibrium with each other as a function of the aqueous solution pH value and the temperature. In fact, the examination of low temperature EPR spectra at pH near 7 revealed not only a square-based pyramid complex but also products of decomposition. These results were also confirmed by the trend found in the formal redox potentials by the voltammetric measurements on many of these ternary complexes.

## 1. Introduction

In the last few years, in spite of scientific progress, the number of cancer cases has risen in a worrying trend, making cancer one of the leading causes of death. For this reason during the past many efforts were made in order to potentially find new drugs which could be more effective in the therapy against this disease. One of the well-known and widely used metal-based drug for chemotherapy is cisplatin [1–4] whose effectiveness unfortunately has limitations due to its side effects, as high toxicity and low administration dosage. Therefore, in order to find a suitable alternative to this drug, a number of transition metal complexes have been synthesized and tested as chemotherapeutic drugs, including copper complexes.

It is well known that copper is an essential trace element playing a significant role in biological systems and its complexes have been studied in order to find a treatment for various diseases, such as Menkes', Wilson's, Alzheimer's, Parkinson's, prion diseases, in which a significant *dyshomeostasis* of copper has been detected [5].

Furthermore, in the past decades several studies demonstrated how some copper(II) complexes, in particular those including 2,2'-bipyridine (bipy) or 1,10-phenanthroline (phen), are able to bind to DNA in a partial intercalative interaction at its minor groove, showing DNA cleavage activity [6,7]. For these reasons, these complexes have been

studied as antitumor agents and their cytotoxic properties have been investigated on tumor cell lines, such as human colon cancer and breast cancer cells or nasopharyngeal carcinoma, and they are known as *casiopeinas* [8–10].

Among these complexes what attracted much attention over the years are ternary metal complexes involving the heterocyclic diimine, 1,10-phenanthroline, as primary ligand, and various biomolecules like aminoacidates, as secondary ligand. Therefore, many efforts have been dedicated to synthesize and characterize these ternary copper(II) complexes. Most scientific works deal with their solid state structure determined by means of X-ray diffraction studies, which very often show a distorted square pyramidal geometry [11–14]. Now most of these interaction studies with DNA were investigated through UV–Vis absorption and fluorescence spectra in aqueous solution, as well as the SOD-like activity determined using the method of nitro blue tetrazolium (NBT) photoreduction [15–21].

In this scenario we wanted to explore the aqueous solution copper (II) complex geometries exhibited by the ternary copper complexes containing 1,10-phenanthroline, as primary ligand, and various aminoacidates, as secondary ligand, to verify if their coordination geometry observed at solid state is maintained. In order to reach this goal, copper (II) complexes were prepared in situ and their UV–Vis–NIR and EPR spectroscopic features as well as their formal reduction potentials were

\* Corresponding author.

E-mail address: [rbonomo@unict.it](mailto:rbonomo@unict.it) (R.P. Bonomo).

<https://doi.org/10.1016/j.jinorgbio.2018.10.012>

Received 16 July 2018; Received in revised form 18 October 2018; Accepted 29 October 2018

Available online 03 November 2018

0162-0134/ © 2018 Elsevier Inc. All rights reserved.

used to gain information about their peculiar molecular geometries and chemical behaviour in aqueous solution.

## 2. Materials and methods

### 2.1. Preparation of copper complexes *in situ*

L-arginine (Arg), L-aspartic acid (Asp), L-histidine (His), L-glutamic acid (Glu), L-glutamine (Gln), L-leucine (Leu), L-lysine (Lys), L-methionine (Met), L-phenylalanine (Phe), L-tryptophan (Trp), L-tyrosine (Tyr), L-Valine (Val) and 1,10-phenanthroline (phen) were purchased from Sigma-Aldrich and were used as received. Ternary copper(II) complexes (charges were often omitted for the sake of simplicity) were prepared by addition of the appropriate amount of isotopically pure  $^{63}\text{Cu}(\text{NO}_3)_2$  50 mM to an aqueous solution containing the pertinent aminoacidate (AA) and phen, with metal to ligand ratios Cu:phen:AA ranging from 1:1:1 up to 1:1:1.1, respectively. A slight excess of AA was used to favour the ternary complex formation. The absolute copper concentration ranged from 1 to 4 mM. The final aqueous solution pH was adjusted by means of a Orion 9103SC combined glass microelectrode connected to a Orion Star A 211 pH meter to pH values comprised in the range 6.5–7.5 by using concentrated NaOH or  $\text{HNO}_3$  as required and stirring the solution for at least 10 min in order to favour the copper mixed species formation. Only in the case of L-histidine the copper ternary complex was examined both in slight acidic (pH = 4.5–5.0) and neutral solutions (pH = 6.5–7.5) and always freshly prepared solutions were analyzed. Previous pHmetric studies (from which complex species distribution diagrams can be obtained as a function of the solution pH) have shown that at pH values higher than 5 the copper ternary complex with phen and AA is the most abundant with a complex formation percentages > 80%, whilst other minor complex species reach < 10% formation [22–31]. Some species distribution diagrams, obtained by using  $\log\beta$  values reported in the above-cited references, will be shown in the Results and Discussion section. Generally, minor species do not contribute to the overall RT or LT EPR spectra because they are relegated to instrumental noise; nevertheless they could have a little influence on the  $\lambda_{\text{max}}$  of the visible absorption spectrum.

### 2.2. CW EPR measurements

A Bruker Elexsys E500 CW-EPR spectrometer driven by a PC running XEpr program under Linux and equipped with a Super-X microwave bridge operating at 9.3–9.9 GHz and a SHQE cavity was used throughout this work. All the EPR spectra of frozen solution of copper (II) complexes were recorded in quartz tubes at 150 K by means of a ER4131VT variable temperature apparatus, also controlling all the RT or LT experiments at variable temperature. The measurements at room temperature were also recorded by means of a WG-812-H flat quartz cell. In the case of RT EPR spectra, the isotropic magnetic parameters were evaluated from the average distances among the four peaks of the experimental spectra recorded in the 2nd derivative mode.

Methanol or glycerol up to 10% was added to the aqueous solution containing the ternary species in order to increase resolution of the LT frozen solution spectra. EPR anisotropic magnetic parameters were obtained directly from the experimental EPR spectra, calculating them from the 2nd and the 3rd line to get rid of second order effects [32]. Perpendicular parameters were obtained exploiting the appearance of the extra-peak due to the angular anomaly, whose field can be used in connection with the parallel parameters to calculate with a certain accuracy  $g_{\perp}$  and  $A_{\perp}$  as explained in the literature [33,34]. In the cases in which simulations of the LT EPR spectra were produced a modified program from J. R. Pilbrow et al. [35] was used.

Instrumental settings of frozen solution EPR spectra recording were as following: number of scans 1–3, microwave frequency 9.46–9.48 GHz, modulation frequency 100 kHz, modulation amplitude

0.2–0.6 mT, time constant 164–327 ms, sweep time 3–6 min, microwave power 10–15 mW, linear receiver gain  $1 \times 10^4$ – $1 \times 10^5$ . Instrumental settings of room temperature solution EPR spectra were substantially the same except for the value of microwave frequency which was in the range 9.70–9.80 GHz, when using the flat quartz cell and microwave power up to 40 mW. Additionally, sometimes > 10 scans were acquired to achieve a good signal to noise ratio.

### 2.3. UV-Vis-NIR measurements

Optical absorption spectra in the UV-Vis-NIR region were collected at room temperature with a Jasco V-770 spectrophotometer in 1 cm path length quartz cells. For the visible and near infrared regions the complex aqueous solutions were those used for the RT and LT EPR study, whilst for the UV region 20 mM solutions of the copper ternary complexes were prepared using the above-described ratios of  $\text{Cu}(\text{NO}_3)_2$  (in its natural isotopic abundance), phen and AA in the same pH range.

### 2.4. Voltammetric measurements

Cyclic voltammograms (CVs) of these Cu(II) complexes in 0.1 M  $\text{KNO}_3$  (as ground electrolyte) aqueous solution in the same copper and ligand concentrations used in the spectroscopic study were recorded by means of a Metrohm Autolab PGSTAT 204 potentiostat-galvanostat driven by a standard PC. They were analyzed by using a Metrohm glass cell with a three electrodes assembly: a working glassy carbon electrode (2 mm diameter), a platinum rod as auxiliary electrode and an Ag/AgCl reference electrode. All electrodes and parts were manufactured by Metrohm. Complex solutions were purged by using ultrapure nitrogen gas. Electrochemical measurements were generally acquired in the region from  $-0.100$  to  $-0.900$  V. The Square Wave Voltammetry (SWV) experiments were carried out on the same solutions at a 25 Hz frequency and a 25–35 mV applied pulse value, avoiding more intense pulses which can cause broadening of the current peak and were carried out at 25 °C. All potentials in the paper are referred to Ag/AgCl reference electrode, +0.215 V vs. Normal Hydrogen Electrode (NHE), unless otherwise stated. The Ag/AgCl electrode potential was checked by using methylviologen redox couple ( $\text{MV}^{2+}/\text{MV}^{+}$ )  $-0.446$  V vs. NHE [36].

## 3. Results and discussion

### 3.1. EPR spectra

First, for the sake of simplicity it is better to discuss RT and LT EPR spectra of all the ternary copper(II) complexes with phen and AA except for the case of histidine, whose behaviour deserves relevant and pertinent comments that will be discussed later. Fig. 1 reports, as example, two species distribution diagrams drawn out for  $[\text{Cu}(\text{phen})(\text{t-Tyr})]$  and  $[\text{Cu}(\text{phen})(\text{t-Leu})]$  systems on the basis of the  $\log\beta$  values reported in the work of N. Turkel and Ç. Şahin [23] and D. İnci and R. Aydm [24]. As it is possible to see, the formation of ternary species in both cases reaches > 80% of the total copper. This behaviour is the same for all the other ternary copper(II) complexes examined in this paragraph.

Actually, the frozen solution EPR spectra of all these ternary complexes with phen and AA do not present remarkable differences: all show one single signal coming from the copper(II) ternary complex,  $[\text{Cu}(\text{phen})(\text{AA})]^+$ . Their anisotropic magnetic parameters are reported in Table 1, together with their isotropic magnetic parameter obtained from RT EPR spectra. These latter spectra, recorded as 2nd derivative spectra, show a remarkable shf structure (superimposed to the highest field line) consisting of seven clearly visible lines due to the interaction of copper(II) free electron with the nuclei of three nitrogen donor atoms in its equatorial coordination plane, as illustrated in Fig. 2. When three quasi equivalent nitrogen atoms are coordinated to copper a pattern showing seven shf lines (with intensity distribution 1:3:6:7:6:3:1) might be

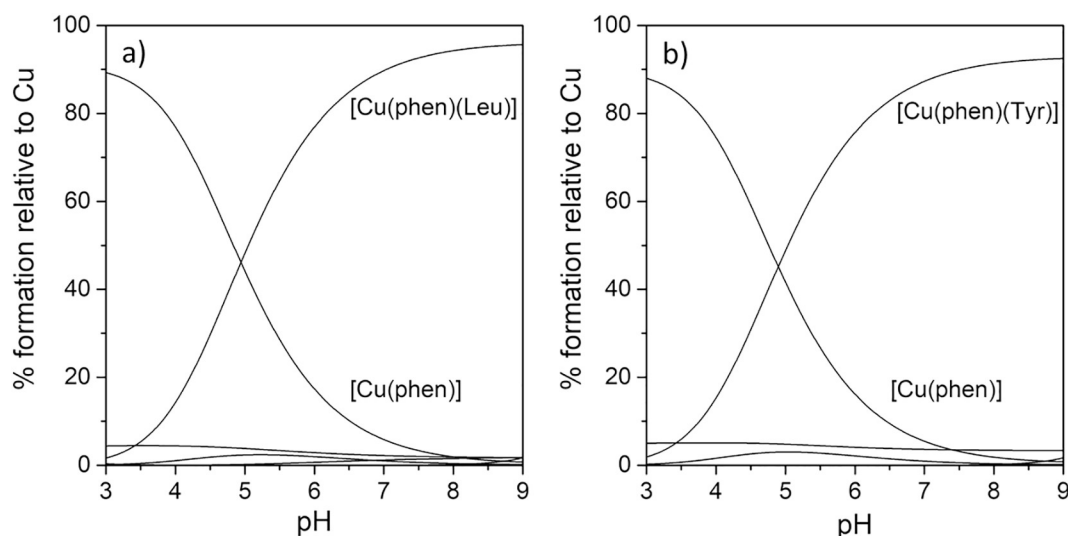


**Fig. 1.** Species distribution diagrams of the (a) [Cu(phen)(L-Tyr)] and (b) [Cu(phen)(L-Leu)] systems obtained considering Cu:phen:AA ratios 1:1:1 and the concentration of initial copper 1 mM. Other minor species < 10% in (a) are free Cu, [Cu(Tyr)], [Cu(Tyr)<sub>2</sub>], [Cu(phen)<sub>2</sub>] and in (b) free Cu, [Cu(Leu)], [Cu(Leu)<sub>2</sub>], [Cu(phen)<sub>2</sub>]. Charges are omitted for simplicity.

reasonably expected [37]. As it is possible to verify the average values of the spin Hamiltonian parameters are all practically identical with negligible differences, always falling within the experimental error ( $g_{\text{iso}} = 2.121 \pm 0.002$ ,  $a_{\text{iso}} = 70 \pm 2 \times 10^{-4} \text{ cm}^{-1}$ ,  $g_{\parallel} = 2.240 \pm 0.003$ ,  $A_{\parallel} = 187 \pm 3 \times 10^{-4} \text{ cm}^{-1}$ ,  $g_{\perp} = 2.051 \pm 0.003$ ,  $A_{\perp} = 12 \pm 3 \times 10^{-4} \text{ cm}^{-1}$ ).

Fig. 3 presents the frozen solution EPR spectrum of the ternary copper(II) complex with phen and Tyr, in which it is possible to note the extra-peak in the perpendicular region, which has been often confused for a rhombic anisotropy in the literature [38]. The inset shows the well resolved  $A_{\perp}^N$  [39] structure on the parallel lowest field line. All these frozen solution EPR spectra are characterized from  $g_{\parallel} > g_{\perp} > 2.040$ , therefore indicating that all these ternary copper(II) complexes have a copper  $d_{x^2-y^2}$  or  $d_{xy}$  ground state, typical for octahedral, square-base pyramidal or square planar stereochemistries [40]. Since the absolute values of parallel hyperfine constants are not so large to consider square planar geometries or so low to take into account square-based pyramids (mixing of the  $3d_z^2$ ,  $4s$  and  $4p$  orbitals into the copper ground state generally provokes a decrease of the magnitude of the resulting hyperfine interaction), the tetragonally elongated octahedron should be the preferential geometry for these copper mixed complexes probably having oxygen donor atoms from water molecules apically bound [41].

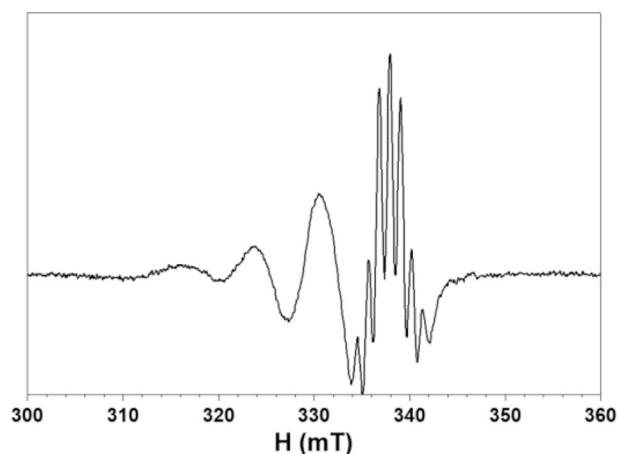


**Fig. 2.** RT EPR 2nd derivative spectrum of the ternary copper complex with L-leucine and 1,10-phenanthroline in aqueous solution at pH 6.5–7. All the copper ternary complexes with the other aminoacids ligands gave rise to the same pattern in their RT EPR spectra.

**Table 1**

Spin Hamiltonian parameters of ternary copper(II) complexes with 1,10-phenanthroline and aminoacids at pH = 6.5–7.5, drawn out from frozen solution and RT EPR spectra.

Copper complexes <sup>a</sup>	$g_{\text{iso}}$ (2)	$a_{\text{iso}}$ (2)	$g_{\parallel}$ (3)	$A_{\parallel}$ (3)	$g_{\perp}$ (5)	$A_{\perp}$ (5)	$a_{\text{iso}}^N$ (1)	$A_{\perp}^N$ (1)	$A_{\parallel}^N$ (1)
[Cu(phen)(L-Arg)] <sup>+</sup>	2.121	71	2.240	188	2.052	12	10	–	11
[Cu(phen)(L-Asp)] <sup>+</sup>	2.122	72	2.242	187	2.053	10	10	–	11
[Cu(phen)(L-Glu)] <sup>+</sup>	2.119	70	2.242	186	2.050	11	10	–	12
[Cu(phen)(L-Gln)] <sup>+</sup>	2.122	71	2.241	186	2.048	13	11	–	12
[Cu(phen)(L-Leu)] <sup>+</sup>	2.122	71	2.241	187	2.049	11	10	–	11
[Cu(phen)(L-Lys)] <sup>+</sup>	2.119	70	2.240	187	2.051	14	10	–	11
[Cu(phen)(L-Met)] <sup>+</sup>	2.122	72	2.241	186	2.049	11	10	–	11
[Cu(phen)(L-Phe)] <sup>+</sup>	2.121	70	2.238	186	2.053	10	10	–	11
[Cu(phen)(L-Trp)] <sup>+</sup>	2.122	71	2.237	188	2.054	11	10	–	11
[Cu(phen)(L-Tyr)] <sup>+</sup>	2.121	71	2.241	184	2.050	14	10	10 <sup>b</sup>	11
[Cu(phen)(L-Val)] <sup>+</sup>	2.119	70	2.240	188	2.051	14	10	–	11

<sup>a</sup> All the hyperfine coupling constants are expressed in  $10^4 \text{ cm}^{-1}$  unit.  $A_{\perp}^N$  would be better represented by  $1/2(A_{\parallel}^N + A_{\perp}^N)$  as explained in ref. [39]. Values between brackets represent the estimated error on the last decimal figure.

<sup>b</sup> Value obtained only for the copper(II) ternary complex with Tyr. In all the other ternary complexes the parallel nitrogen shf structure was not clearly resolved.

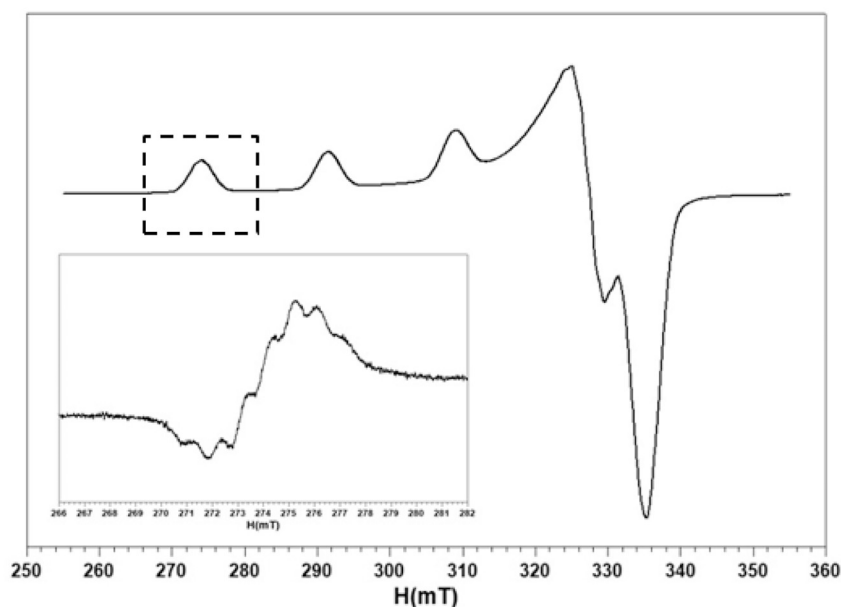


Fig. 3. LT EPR spectrum of the copper ternary complex with L-tyrosine and 1,10-phenanthroline in aqueous solution at pH 6.5–7.0. The inset contains an enlarged view of the seven-lines superhyperfine structure superimposed on the lowest field feature recorded in the 2nd derivative mode.

### 3.2. UV–Vis–NIR spectra

The same considerations can be made looking at the UV–Vis–NIR absorption spectra, whose experimental results are reported in Table 2. The d-d bands and the CT transitions fall within the same wavelength regions and show similar molar extinction coefficients. The slight oscillation around the  $\lambda_{\text{max}}$  value of the broad band in the visible region could be due to different constraints exerted by the different aminoacids on the copper coordination plane. Additionally, the presence of minor complex species (as said above in the Section 2.1), which form in the same pH region, could contribute to the overall absorption envelope. In any case the  $\lambda_{\text{max}}$  value, centred around 610–620 nm due to the promotion of low energy d electrons to the  $d_{x^2-y^2}$  hole, is the value expected for a  $\text{CuN}_3\text{O}$  in plane chromophore [42]. The two weak CT transitions result from electron transfer from ligand to metal (therefore LMCT) and, in particular, from  $\sigma\text{N}$  to the  $\text{Cu(II)} d_{x^2-y^2}$  orbital along the Cu–N bond [41]. Other very intense bands in the UV region 250–300 nm are present in all the absorption spectra of these copper ternary complexes and they are ascribable to  $\pi \rightarrow \pi^*$  intra-ligand transitions. All these results are not really different from those previously reported in the literature by slightly changing the experimental conditions [43,44].

Evidently the similarity of the UV–Vis–NIR and EPR spectroscopic data associated with these ternary copper(II) complexes containing both phen and AA suggests that all these complex species have a unique

Table 2

Average data from UV–Vis–NIR absorption spectra of ternary copper(II) complexes with 1,10-phenanthroline and aminoacids at pH = 6.5–7.5.

Copper complexes <sup>a</sup>	d–d band	$\epsilon$ ( $\text{M}^{-1} \text{cm}^{-1}$ )	CT bands	$\epsilon$ ( $\text{M}^{-1} \text{cm}^{-1}$ )
	$\lambda_{\text{max}}$ (nm)			
[Cu(phen)(AA)] <sup>+</sup>	618 ± 6	57 ± 5 <sup>b</sup>	328 ± 4	1000 <sup>d</sup>
		72 ± 4 <sup>c</sup>	304 ± 3	4000 <sup>d</sup>

<sup>a</sup> AA abbreviation stands for L-Arg, L-Asp, L-His, L-Glu, L-Gln, L-Leu, L-Lys, L-Met, L-Phe, L-Trp, L-Tyr, L-Val.

<sup>b</sup> Molar extinction coefficient for AA having aliphatic chain residues.

<sup>c</sup> Molar extinction coefficient for AA having aromatic chain residues.

<sup>d</sup> Errors in CT molar extinction coefficients were evaluated to be around 15%.

molecular shape in aqueous solution, that is a pseudo-octahedral geometry (the usual copper tetragonally elongated octahedron) with a  $\text{CuN}_3\text{O}$  in plane chromophore and two water apically bound.

### 3.3. Copper(II) ternary complexes with phen and L-His

Histidine behaves differently, because it is well known its ability to coordinate copper in a glycine-like fashion at pH values in which the imidazole group is still protonated and histamine-like at slightly higher pH values in which the imidazole group deprotonates because of the presence of copper. The overall picture could be actually a little more complicated by the fact that minor mono- and bis-complex species coming from phen and histidine could be contemporary present in the system, even if previous pHmetric studies tend to exclude this possibility when working with metal to ligand ratios Cu:phen:AA about 1:1:1. Actually a species distribution diagram is shown in Fig. 4 and it

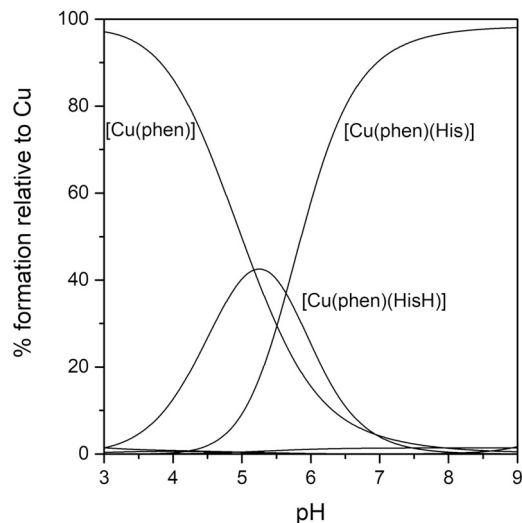


Fig. 4. Species distribution diagram of the [Cu(phen)(L-His)] system obtained considering Cu:phen:His ratio equal to 1:1:1 and the concentration of initial copper was 1 mM. Other minor species < 10% are free Cu, [Cu(His)], [Cu(HisH)]. Charges are omitted for simplicity.

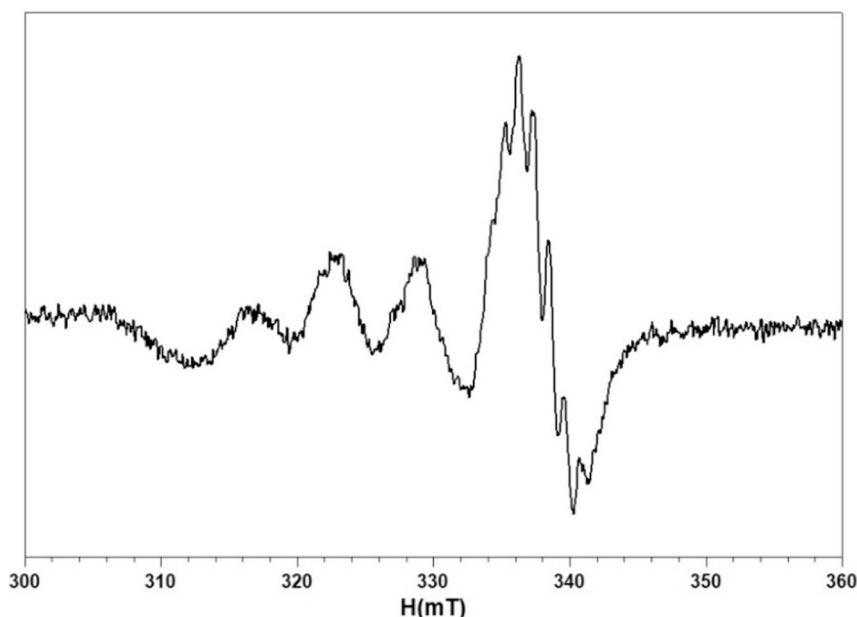


Fig. 5. RT EPR 2nd derivative spectrum of a 3 mM aqueous solution of the copper ternary complex with L-histidine and 1,10-phenanthroline in the metal to ligands ratio 1:1:1 at pH 5 after having subtracted the contribution of the copper 1,10-phenanthroline mono complex evaluated to be about 35% of the total copper.

was obtained by using the  $\log\beta$  values from the previous work of V. K. Patel, P.K. Bhattacharya [22].

A RT EPR spectrum in the second derivative mode on a sample containing copper(II), phen and His in 1:1:1 metal to ligands ratios at pH value of 5.0 is shown in Fig. 5 and presents the following parameters:  $g_{\text{iso}} = 2.120(2)$ ,  $a_{\text{iso}} = 68(2) \times 10^{-4} \text{ cm}^{-1}$ ,  $a_{\text{iso}}^{\text{N}} = 10(1) \times 10^{-4} \text{ cm}^{-1}$ . This RT EPR spectrum, ascribable to  $[\text{Cu}(\text{phen})(\text{HisH})]$  species, was obtained by subtracting the RT EPR spectrum of the simple  $[\text{Cu}(\text{phen})]^{2+}$  complex in the proper percentage according to the species distribution diagram reported in Fig. 4. The structure of seven shf lines can be easily observed superimposed on the highest field line, therefore implying that three nitrogen donor atoms are involved in the equatorial coordination sphere of copper.

LT EPR spectra for the copper ternary system with phen and His have to be run by adding glycerol up to 10% because the addition of methanol in this system did not improve the spectral resolution and very broad spectra were generally obtained up to water-methanol mixtures 30–70%. The LT spectrum at pH 5 (see Fig. 6) obviously presents two absorbing species: the simple copper complex  $[\text{Cu}(\text{phen})]$  and ternary complex  $[\text{Cu}(\text{phen})(\text{HisH})]$ . The first one presents these parameters:  $g_{\parallel} = 2.310(3)$ ,  $A_{\parallel} = 162(3) \times 10^{-4} \text{ cm}^{-1}$ ,  $g_{\perp} = 2.067(5)$ ,  $A_{\perp} = 8(5) \times 10^{-4} \text{ cm}^{-1}$ . They are not dissimilar from those reported in the literature even if it is not always clear whether authors used isotopically pure copper or not [45].  $[\text{Cu}(\text{phen})(\text{HisH})]$  shows a frozen EPR spectrum similar to those of the other copper(II) ternary complexes with the following parameters:  $g_{\parallel} = 2.240(3)$ ,  $A_{\parallel} = 187(3) \times 10^{-4} \text{ cm}^{-1}$ ,  $g_{\perp} = 2.053(5)$ ,  $A_{\perp} = 11(5) \times 10^{-4} \text{ cm}^{-1}$ . Hence, at relatively acidic pH values the coordination environment around copper is not different from that of the other copper(II) ternary complexes so far examined, namely even for the ternary complex with phen and His a pseudo-octahedral geometry with a  $\text{CuN}_3\text{O}$  in plane chromophore easily forms.

The situation is completely different when the pH value is raised up to the neutral region. The RT spectrum recorded at room temperature do not show resolved shf lines due to coordinated nitrogen atoms (see Fig. 7) and, moreover, the isotropic spin Hamiltonian parameters are quite different from those determined at pH 5 ( $g_{\text{iso}} = 2.125(2)$ ,  $a_{\text{iso}} = 60(2) \times 10^{-4} \text{ cm}^{-1}$ ).

Unfortunately the LT EPR spectrum is not conclusive (see Fig. 8) because it shows more than one absorbing species and furthermore the

most intense signal presents the same magnetic parameters of the ternary complex obtained at pH 5, which means that the formation of the two copper ternary complexes,  $[\text{Cu}(\text{phen})(\text{HisH})]^+$  and  $[\text{Cu}(\text{phen})(\text{His})]^+$  respectively, is dependent on the temperature in a different way. The former is probably enthalpically favoured so that low temperatures favour its formation. On the contrary, the formation of the latter might be an endothermic process, so that at low temperatures its formation is disfavoured and this is the reason why is relegated to a minor species. Fig. 8a presents the entire LT spectrum (run at the temperature of 140 K) with the attempt of a simulation by considering the presence of three absorbing complex species in the system. The first signal has very similar parameters of the complex species  $[\text{Cu}(\text{phen})(\text{HisH})]^+$  at pH 5 with a weight of about 38% ( $g_{\parallel} = 2.239(4)$ ,  $A_{\parallel} = 184(3) \times 10^{-4} \text{ cm}^{-1}$ ,  $g_{\perp} = 2.054(5)$ ,  $A_{\perp} = 9(5) \times 10^{-4} \text{ cm}^{-1}$ ). The other two absorbing species are associated with two different copper complex species: one of them, with a weight of about 45%, has magnetic parameters  $g_{\parallel} = 2.306(5)$ ,  $A_{\parallel} = 162(3) \times 10^{-4} \text{ cm}^{-1}$ ,  $g_{\perp} = 2.068(5)$ ,  $A_{\perp} = 7(5) \times 10^{-4} \text{ cm}^{-1}$ ; the other one, with a weight of about 17%,  $g_{\parallel} = 2.282(5)$ ,  $A_{\parallel} = 173(3) \times 10^{-4} \text{ cm}^{-1}$ ,  $g_{\perp} = 2.064(5)$ ,  $A_{\perp} = 8(5) \times 10^{-4} \text{ cm}^{-1}$ .

At first sight, these two copper complex species might be considered disproportion products of the ternary complex  $[\text{Cu}(\text{phen})(\text{His})]$ , namely  $[\text{Cu}(\text{phen})_2]^{2+}$  and  $[\text{Cu}(\text{His})_2]$ . Unfortunately, the average magnetic parameters reported in the literature for the copper bis complex species with Phen and His are completely different and, in particular, for the former [46,47]  $g_{\parallel} = 2.280(5)$ ,  $A_{\parallel} = 164(4) \times 10^{-4} \text{ cm}^{-1}$ ,  $g_{\perp} = 2.070(5)$ ,  $A_{\perp} = 29(5) \times 10^{-4} \text{ cm}^{-1}$  and for the latter [45,48–50]  $g_{\parallel} = 2.228(8)$ ,  $A_{\parallel} = 185(5) \times 10^{-4} \text{ cm}^{-1}$ ,  $g_{\perp} = 2.050(6)$ ,  $A_{\perp} = 13(5) \times 10^{-4} \text{ cm}^{-1}$ . Thus, this first hypothesis must be excluded. However, the most abundant copper species, found by simulating the LT EPR spectrum (45%), has actually identical magnetic parameters of the  $[\text{Cu}(\text{phen})]^{2+}$  complex, therefore the ternary  $[\text{Cu}(\text{phen})(\text{His})]^+$  complex dissociates at low temperature. About the other two species, one (38%) might be the same ternary complex obtained at pH 5; the other one (17%) a square-based pyramidal complex (namely properly  $[\text{Cu}(\text{phen})(\text{His})]^+$ ), in which histidine probably coordinates copper with its histamine-like mode. The higher  $g$  parallel value,  $g_{\parallel} = 2.282(5)$ , and the relatively lower parallel hyperfine constant,  $A_{\parallel} = 173(3) \times 10^{-4} \text{ cm}^{-1}$ , in comparison with the magnetic parameters of  $[\text{Cu}(\text{phen})(\text{HisH})]^+$ , tend to confirm this conclusion.

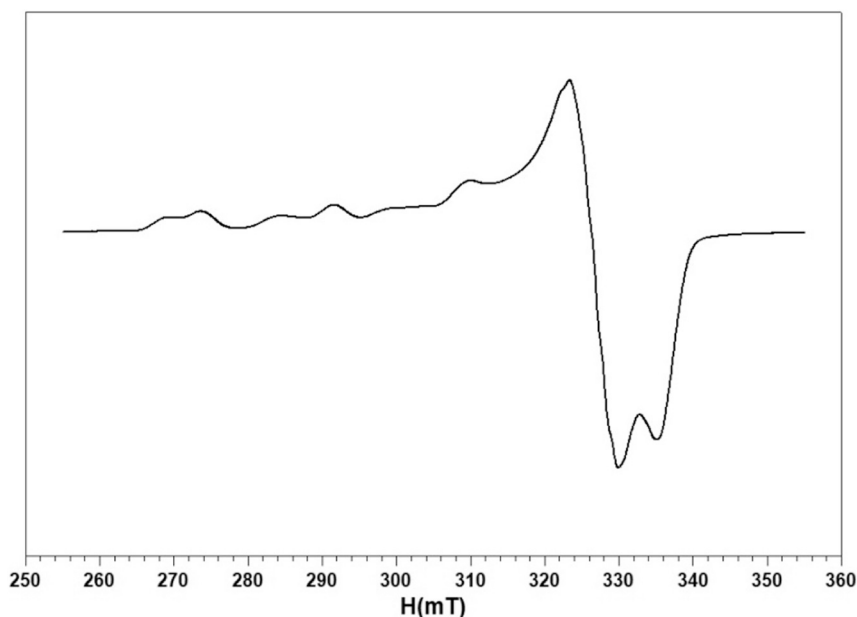
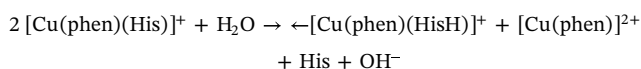
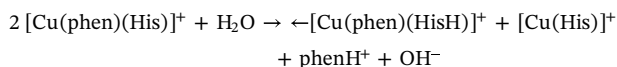


Fig. 6. LT EPR spectrum of a 3 mM aqueous solution of the copper ternary complex with L-histidine and 1,10-phenanthroline in the metal to ligands ratio 1:1:1 respectively at pH 5.

Therefore our interpretation is that the copper ternary complex  $[\text{Cu}(\text{phen})(\text{His})]^+$  is stable only at room temperature and that low temperatures disfavour its existence. There is an equilibrium between  $[\text{Cu}(\text{phen})(\text{HisH})]^+$  and  $[\text{Cu}(\text{phen})(\text{His})]^+$  that is a function of the temperature, complicated by a side dissociation reaction:



This side reaction could also involve the dissociation of His from the copper ternary complex:



Actually copper mono His complex species has magnetic parameters quite similar to those of the  $[\text{Cu}(\text{phen})]^{2+}$  species ( $g_{\parallel} = 2.310$ ,  $A_{\parallel} = 170 \times 10^{-4} \text{ cm}^{-1}$ ,  $g_{\perp} = 2.070$ ) [51,52]; moreover, both dissociation processes could occur simultaneously. This might be the reason why the second signal is the most intense due to both contributions. Analogous information can be obtained by examining the UV-Vis-NIR absorption spectra. The visible absorption spectra show different  $\lambda_{\text{max}}$ : at pH = 5.0, 650(6) nm with  $\epsilon (\text{M}^{-1} \text{ cm}^{-1}) = 48(7)$ ; at pH 7.0, 677(4) nm with  $\epsilon (\text{M}^{-1} \text{ cm}^{-1}) = 87(4)$ . CT transitions occur always at the same wavelength values.

All these results taken together lead to the conclusion that the  $[\text{Cu}(\text{phen})(\text{His})]^+$  species has a different stereochemistry, as we have said before in the discussion of the LT EPR spectra. In particular, at room temperature the relatively higher  $g_{\text{iso}}$  and the smaller absolute value of

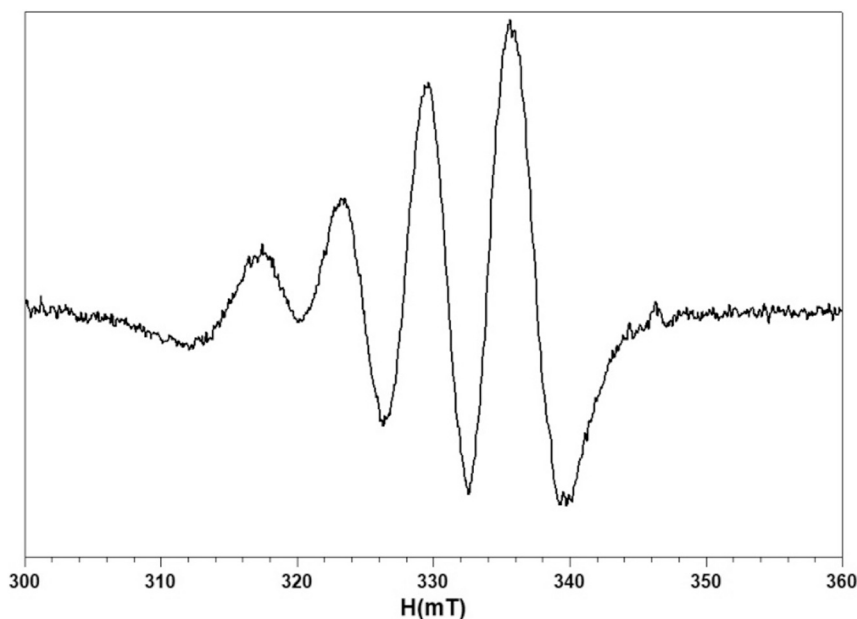
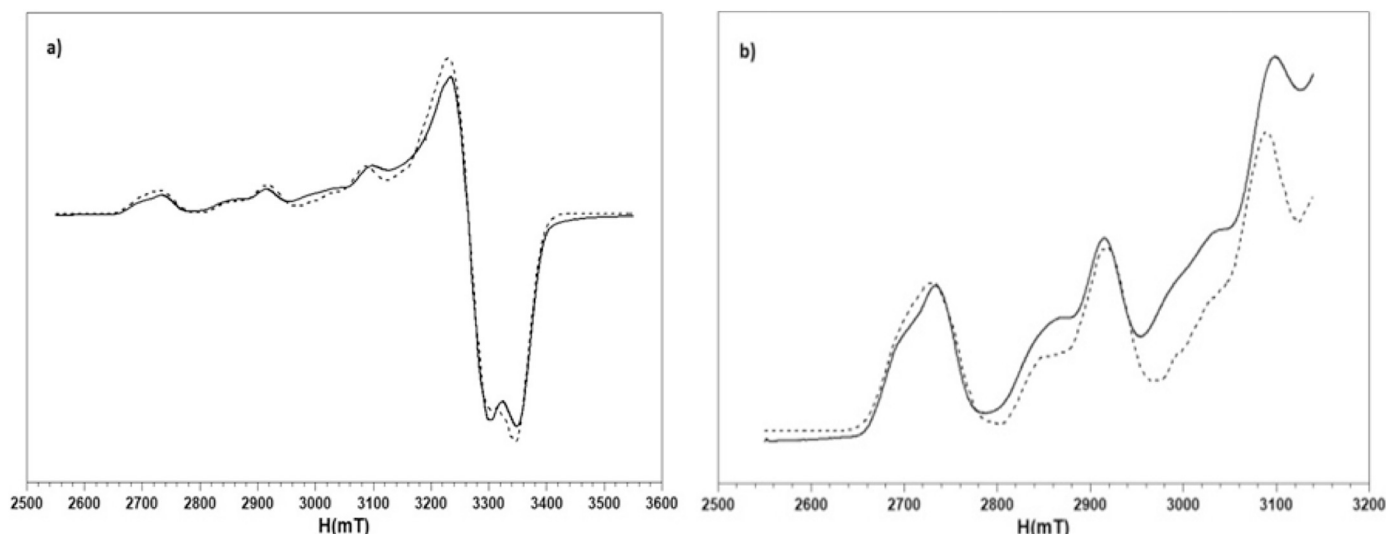
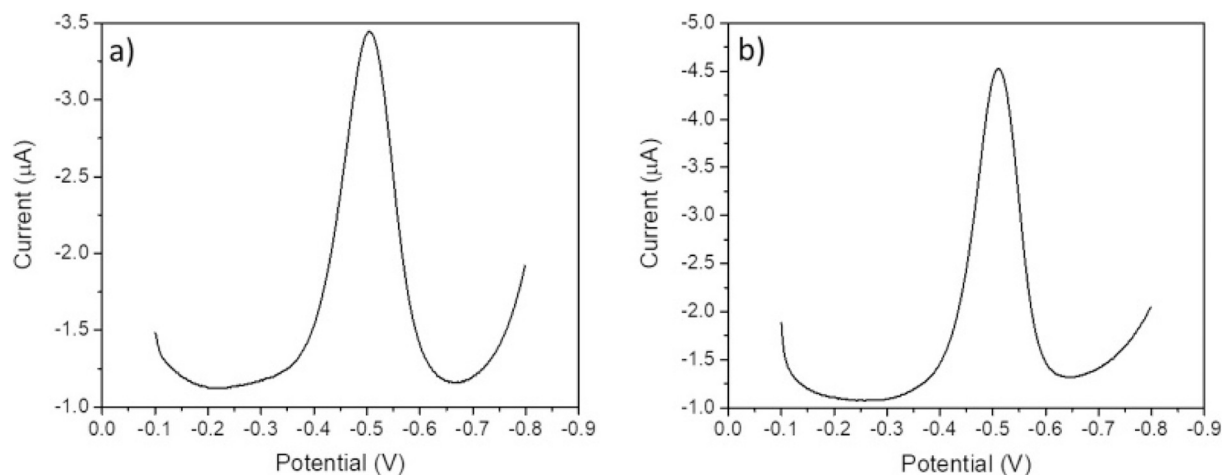


Fig. 7. RT EPR 2nd derivative spectrum of a 3 mM aqueous solution of the copper ternary complex with L-histidine and 1,10-phenanthroline in a metal to ligands ratio 1:1:1 respectively at pH 7.



**Fig. 8.** Frozen solution EPR spectrum of a 3 mM aqueous solution of the copper ternary complex with L-histidine and 1,10-phenanthroline in a metal to ligands ratio 1:1:1 respectively at pH 7. The dotted spectrum represents the best simulation a) of the entire spectrum and b) of the parallel part obtained with the following magnetic parameters: 38%  $g_{||} = 2.239(4)$ ,  $A_{||} = 184(3) \times 10^{-4} \text{ cm}^{-1}$ ,  $g_{\perp} = 2.054(5)$ ,  $A_{\perp} = 9(5) \times 10^{-4} \text{ cm}^{-1}$ , 45%  $g_{||} = 2.304(5)$ ,  $A_{||} = 162(3) \times 10^{-4} \text{ cm}^{-1}$ ,  $g_{\perp} = 2.068(5)$ ,  $A_{\perp} = 7(5) \times 10^{-4} \text{ cm}^{-1}$  17%  $g_{||} = 2.282(5)$ ,  $A_{||} = 173(3) \times 10^{-4} \text{ cm}^{-1}$ ,  $g_{\perp} = 2.064(5)$ ,  $A_{\perp} = 8(5) \times 10^{-4} \text{ cm}^{-1}$ .



**Fig. 9.** Square wave voltammograms of the copper ternary species with phen and a) L-Asp or b) L-Leu in aqueous solution at neutral pH with 0.1 M  $\text{KNO}_3$  as ground electrolyte.

**Table 3**

SQW formal redox potentials of ternary copper(II) complexes with 1,10-phenanthroline and aminoacids at pH = 6.5–7.5, in aqueous solution by using  $\text{KNO}_3$  0.1 M as background electrolyte. PWHH is the abbreviation of peak width at half height. Presumed errors are reported between brackets.

Copper complexes <sup>a</sup>	pH	$E_p$ , mV, Ag/AgCl (12 mV)	PWHH, mV (10 mV)
$[\text{Cu}(\text{phen})(\text{L-Arg})]^+$	7.2	-363	200
$[\text{Cu}(\text{phen})(\text{L-Lys})]^+$	7.4	-354	170
$[\text{Cu}(\text{phen})(\text{L-Asp})]^+$	7.2	-503	110
$[\text{Cu}(\text{phen})(\text{L-Leu})]^+$	7.0	-510	93
$[\text{Cu}(\text{phen})(\text{L-Phe})]^+$	7.2	-488	227
$[\text{Cu}(\text{phen})(\text{L-Trp})]^+$	7.1	-498	235
$[\text{Cu}(\text{phen})(\text{L-Tyr})]^+$	7.0	-496	195
$[\text{Cu}(\text{phen})(\text{L-His})]^+$	5.0	-164	84
		-420	100
$[\text{Cu}(\text{phen})(\text{L-His})]^+$	7.1	-315	125

$a_{\text{iso}}$  as well as the higher  $\lambda_{\text{max}}$  value could lead one to think that a square based pyramidal geometry better represents the coordination environment around copper ion. On the other hand, His together with phen could form a  $\text{CuN}_4$  equatorial chromophore when the former

ligand uses its histamine-like mode of coordination and the carboxylate oxygen atom could be apically bound. Even the molar extinction coefficient plays in favour of this hypothesis: a higher value is generally associated with a metal complex having a lower symmetry [53]. Generally in a square pyramid the metal is tilted out of the equatorial coordination plane and this could explain why the nitrogen shf structure is not resolved (or totally absent) in the RT EPR spectra at pH 7 (Fig. 7).

Some diffractometric results on crystals of  $[\text{Cu}(\text{bipy})(\text{His})]$  showed that at the solid state pentacoordinate copper(II) in an approximate pyramidal structure is simultaneously bound to four nitrogen atoms in a distorted equatorial plane with the carboxylate oxygen atom apically interacting with copper [54]. No diffractometric report on the solid structure of  $[\text{Cu}(\text{phen})(\text{His})]$  is accessible in literature with the exception of a ligand containing phen and His covalently bound to form a copper complex with a distorted square-based pyramidal structure [55].

#### 3.4. Square wave voltammetric results on copper(II) ternary complexes

Carrying out an electrochemical reduction of most of these systems, a mono electronic step can be easily detected, whose re-oxidation is

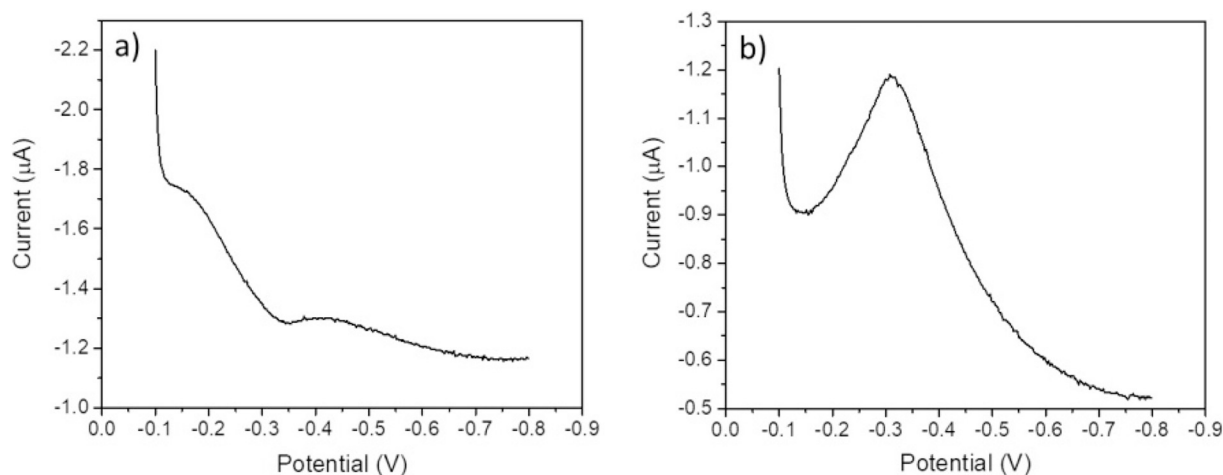


Fig. 10. Square wave voltammograms of the copper ternary species with phen and a) L-His at pH 5 and b) L-His at pH 7 in aqueous solution with 0.1 M  $\text{KNO}_3$  as ground electrolyte.

generally not reversible and leads to decomposition products as it is well recognizable from their cyclic voltammograms (not shown) [56]. In fact, it is well known that the re-oxidation of a copper(I) complex species does not easily yield the previous copper(II) species because of the different geometrical constraints between the Cu(I) and Cu(II) stereochemistries [57]. As shown in Fig. 9, which reports SWV peaks run on solutions containing copper ternary complexes with phen and aminoacids having aromatic or aliphatic residues, the reduction peak occurs generally at negative potentials versus Ag/AgCl reference electrode. As one can see from Table 3, the copper(II) ternary complexes with aromatic residues present a slightly more positive formal redox potential values than those with aliphatic residues. This small difference could be probably ascribed to weak interligand stacking interactions, which are known to be present in these systems [27,58]. Copper (II) ternary complexes with aminoacids carrying positively charged residues also show more positive formal redox potentials. Anyway the substantial negative formal redox potentials found for these ternary copper(II) complexes correlate well with their tetragonally elongated octahedral geometries found in the spectroscopic studies.

A different approach deserves the case of ternary complexes with phen and His because, as it was shown above, different complex species are present as a function of the aqueous solution pH value. Actually, as illustrated in Fig. 10, a different behaviour was obtained at pH values 5 and 7, respectively. At pH 5, as already shown by the species distribution diagram and observed from the pertinent spectroscopic data,  $[\text{Cu}(\text{phen})]$  and  $[\text{Cu}(\text{phen})(\text{HisH})]$  are contemporarily present and the voltammogram shows two peaks associated to the reduction of both complex species.

The more negative SQW peak is ascribable to the reduction of  $[\text{Cu}(\text{phen})(\text{HisH})]^+$  and this value is somewhat in between the formal redox potentials found for aminoacids having charged residues and those pertaining to aromatic residues. At pH 7 a unique SQW peak can be observed (as already suggested by the spectroscopic data at room temperature) and its value is the more positive among the values associated with all the ternary systems examined in this work.

#### 4. Conclusion

In this work EPR and UV–vis data have demonstrated that the ternary copper complexes with phen and several aminoacids in aqueous solution have a unique molecular geometry, that is a tetragonally elongated octahedron with a coordination plane containing the heterocyclic diimine and the aminoacids anion; additionally, two water molecules are apically bound. Unfortunately many studies assume that the diffractometric structural information on single crystals

of copper ternary complexes (which generally adopt distorted square pyramidal coordination geometries with a water molecule apically bound) describes the real copper complex geometry in aqueous solution. We would like to stress with our experimental data that a metal complex stereochemistry found at the solid state not always is preserved when the complex is dissolved in a solvent, especially when the solvent is water the donating ability of which is well-known. The only square pyramidal geometry in aqueous solution among all these aminoacids ligands is probably attributable to the ternary copper complex with phen and His near the neutrality, in which His behaves as terdentate ligand and coordinates by its histamine-like mode.

In the end, we would like to comment that a proper LT EPR spectrum in the case of the ternary complex,  $[\text{Cu}(\text{phen})(\text{His})]^+$  could be only obtained as minor species, because the frozen solution EPR spectrum always revealed the features of  $[\text{Cu}(\text{phen})(\text{HisH})]^+$  and dissociation products  $[\text{Cu}(\text{phen})]^{2+}$  and  $[\text{Cu}(\text{His})]^+$ . Unfortunately, sometimes frozen solution EPR spectra do not refer exactly to the major complex species present at room temperature because the freezing procedure might change the complex species distribution of the system under consideration. In our case dissociation reactions occur and complicate the overall picture too [38].

Furthermore, the voltammetric data also confirm these observations, because only the  $[\text{Cu}(\text{phen})(\text{His})]^+$  complex has the most positive formal redox potential which is ascribable to a square based pyramidal arrangement around copper [57].

#### Acknowledgements

The authors greatly acknowledge University of Studies of Catania for the grant FIR 9DD800. They would also like to express their gratitude to MIUR for the financial support provided by means of PRIN 2015-2015MP34H3 and PRIN2011-E61J12000200001 Research Projects. G. M. thanks for having had the possibility of a three month scholarship within the research themes of CIRCMSB (Consorzio Interuniversitario di Ricerca in Chimica dei Metalli nei Sistemi Biologici), which is also gratefully acknowledged for partially funding our scientific instrumentation.

#### References

- [1] S.D. Williams, R. Birch, L.H. Einhorn, L. Irwin, F.A. Greco, P.J. Loehrer, *N. Engl. J. Med.* 316 (1987) 1435–1440.
- [2] U.E. Studer, M. Bacchi, C. Biedermann, P. Jaeger, R. Kraft, L. Mazzucchelli, R. Markwalder, E.S. Roland, W. Sonntag, *J. Urol.* 152 (1994) 81–84.
- [3] A. Pace, A. Savarese, M. Picardo, V. Maresca, U. Pacetti, G. Del Monte, A. Birocchio, C. Leonetti, B. Jandolo, F. Cognetti, L. Bove, *J. Clin. Oncol.* 21 (2003) 927–931.

- [4] A.M. Florea, D. Büsselberg, *Cancer* 3 (2011) 1351–1371.
- [5] G. Valora, R.P. Bonomo, G. Tabbi, *Inorg. Chim. Acta* 453 (2016) 62–68.
- [6] V.M. Manikandamathavan, R.P. Parameswari, T. Weyhermuller, H.R. Vasanthi, B.U. Nair, *Eur. J. Med. Chem.* 56 (2011) 4537–4547.
- [7] S. Ramakrishnan, V. Rajendiran, M. Palaniandavar, V.S. Periasamy, B.S. Srinag, H. Krishnamurthy, M.A. Akbarsha, *Inorg. Chem.* 48 (2009) 1309–1322.
- [8] A. Hordyjewska, L. Popiolek, J. Kocot, *Biometals* 27 (2014) 611–621.
- [9] T.Y. Han, T.S. Guan, M.A. Iqbal, R.A. Haque, K.S. Rajeswari, M.B.K. Ahamed, A.M.S. Abdul Majid, *Med. Chem. Res.* 23 (2014) 2347–2359.
- [10] Munirah Ahmad, Shazlan-Noor Suhaimi, Tai-Lin Chu, Norazlin Abdul Aziz, Noor-Kaslina Mohd Kornain, D.S. Samiulla, Kwok-Wai Lo, Chew-Hee Ng, Alan Soo-Beng Khoo, *PLoS One* (2018), <https://doi.org/10.1371/journal.pone.0191295>.
- [11] S. Zhang, J. Zhou, *J. Coord. Chem.* 61 (2008) 2488–2498.
- [12] S.R. Liao, X.Y. Le, X.L. Feng, *J. Coord. Chem.* 61 (2008) 847–856.
- [13] P. Santhakumar, M.N. Arumughan, *IJCAS* 3 (2012) 1513–1515.
- [14] P. Jaividhya, R. Dhivya, M.A. Akbarsha, M. Palaniandavar, *J. Inorg. Biochem.* 114 (2012) 94–105.
- [15] X. Le, X. Zhou, C. Huang, X. Feng, *J. Coord. Chem.* 56 (2003) 861–867.
- [16] X. Le, S. Liao, X. Liu, X. Feng, *J. Coord. Chem.* 59 (2006) 985–995.
- [17] B. Annaraj, C. Balakrishnan, M.A. Neelakantan, *J. Photochem. Photobiol. B* 160 (2016) 278–291.
- [18] V.M. Manikandamathavan, R.P. Parameswari, T. Weyhermuller, H.R. Vasanthi, B.U. Nair, *Eur. J. Med. Chem.* 46 (2011) 4537–4547.
- [19] A.K. Patra, S. Dhar, M. Nethaji, A.R. Chakravarty, *Chem. Commun.* (2003) 1562–1563.
- [20] S. Suzuki, K. Yamaguchi, N. Nakamura, Y. Tagawa, H. Kuma, T. Kawamoto, *Inorg. Chim. Acta* 283 (1998) 260–267.
- [21] H. Seng, W. Wang, S. Kong, H. Alan Ong, Y. Win, R. Noor Zaliha, R. Abd Rahman, M. Chikira, W. Leong, M. Ahmad, A. Soo-Beng Khoo, C. Ng, *Biometals* 25 (2012) 1061–1081.
- [22] V.K. Patel, P.K. Bhattacharya, *Inorg. Chim. Acta* 92 (1984) 199–201.
- [23] N. Turkel, Ç. Şahin, *Chem. Pharm. Bull.* 57 (2009) 694–699.
- [24] D. İnci, R. Aydın, *J. Solut. Chem.* 43 (2014) 711–726.
- [25] L.H. Abdel-Rahman, L.P. Battaglia, M.R. Mahmoud, *Polyhedron* 15 (1996) 327–334.
- [26] S. Bandyopadhyay, G.N. Mulkherjee, M.G.B. Drew, *Inorg. Chim. Acta* 359 (2006) 3243–3251.
- [27] O. Yamuchi, A. Odani, *J. Am. Chem. Soc.* 107 (1985) 5938–5945.
- [28] G. Berthon, B. Hacht, M. Blais, P.M. May, *Inorg. Chim. Acta* 125 (1986) 219–227.
- [29] S. Raju, K. Bharath Kumar Naik, B. Ananda Kumar, G. Nageswara Rao, *Chem. Speciat. Bioavailab.* 24 (2012) 46–52.
- [30] A.A. Shoukry, *J. Solut. Chem.* 40 (2011) 1796–1818.
- [31] P. Deschamps, P.P. Kulkarni, M. Gautam-Basak, B. Sarkar, *Coord. Chem. Rev.* 249 (2005) 895–909.
- [32] T. Lund, J. Vanngard, *Chem. Phys.* 42 (1965) 2979–2980.
- [33] R.P. Bonomo, F. Riggi, *Lett. Nuovo Cimento* 30 (1981) 304–310.
- [34] R.P. Bonomo, F. Riggi, *Chem. Phys. Lett.* 93 (1982) 99–102.
- [35] J.R. Pilbrow, M.E. Winfield, *Mol. Phys.* 25 (1973) 1073–1092.
- [36] E. Kaifer, J. Bard, *J. Phys. Chem.* 89 (1985) 4876–4880.
- [37] J.E. Wertz, J.R. Bolton, *Electron Spin Resonance. Elementary Theory and Practical Applications*, Mac Graw Hill, New York, 1972; or N.M. Atherton, *Electron Spin Resonance. Theory and Applications*, Ellis Horwood Limited, Sussex, England, 1973.
- [38] R.P. Bonomo, F. Riggi, A.J. Di Bilio, *Inorg. Chem.* 27 (1988) 2510–2512.
- [39] C.M. Guzy, J.B. Raynor, M.C.M. Symons, *J. Chem. Soc. A* (1969) 2299–2303.
- [40] B.J. Hathaway, D.E. Billing, *Coord. Chem. Rev.* 5 (1970) 143–207.
- [41] B.A. Goodman, J.B. Raynor, *Electron spin resonance of transition metal complexes*, in: H.J. Emeléus, A.G. Sharpe (Eds.), *Adv. Inorg. Chem. Radiochem*, vol. 13, Academic Press, New York, 1970, pp. 135–362.
- [42] A.B.P. Lever, *Inorganic Electronic Spectroscopy*, second edition, Elsevier, New York, 1984, p. 356.
- [43] C. Su, T. Tai, S. Wu, S. Wang, F. Liao, *Polyhedron* 18 (1999) 2361–2368.
- [44] P.S. Subramian, E. Suresh, P. Dastidar, S. Waghmode, D. Srinivas, *Inorg. Chem.* 40 (2001) 4291–4301.
- [45] M. Chikira, Y. Tomizawa, D. Fukita, T. Sugizaki, N. Sugawara, T. Yamazaki, A. Sasano, H. Shindo, M. Palaniandavar, W.E. Antholine, *J. Inorg. Biochem.* 89 (2002) 163–173.
- [46] M.A. Zoroddu, S. Zanetti, R. Pogni, R. Basosi, *J. Inorg. Biochem.* 69 (1996) 291–300.
- [47] T. Hirohama, Y. Kuranuki, E. Ebina, T. Sugizaki, H. Arii, M. Chikira, P. Tamil Selvi, M. Palaniandavar, *J. Inorg. Biochem.* 99 (2005) 1205–1219.
- [48] P. Manikandan, B. Epel, D. Goldfarb, *Inorg. Chem.* 40 (2001) 781–787.
- [49] L. Gala, M. Lawson, K. Jomova, L. Zelenicky, A. Congradyova, M. Mazur, M. Valko, *Molecules* 19 (2014) 980–991.
- [50] R. Basos, G. Valensin, E. Gagelli, W. Froncisz, M. Pasenkiewicz-Gierula, W. Antholine, J. Hide, *Inorg. Chem.* 25 (1986) 3006–3010.
- [51] R. Grommen, P. Manikandan, Y. Gao, T. Shane, J.J. Shane, R.A. Schoonheydt, B.M. Weckhuysen, D. Goldfarb, *J. Am. Chem. Soc.* 122 (2000) 11488–11496.
- [52] D. Baute, D. Arieli, F. Neese, H. Zimmermann, B.M. Weckhuysen, D. Goldfarb, *J. Am. Chem. Soc.* 126 (2004) 11733–11745.
- [53] B.N. Figgis, *Introduction to Ligand Fields*, Interscience Publishers, John Wiley & Sons, Inc, New York, 1966.
- [54] L.H. Abdel-Rahman, L.P. Battaglia, P. Sgarabotto, M.R. Mahmoud, *J. Chem. Crystallogr.* 24 (1994) 567–571.
- [55] S.M.G. Leite, L.M.P. Lima, S. Gama, F. Mendes, M. Orio, I. Bento, A. Paulo, R. Delgado, O. Iranzo, *Inorg. Chem.* 55 (2016) 11801–11814.
- [56] P. Pary, L.N. Bengoa, W.A. Eglı, *J. Electrochem. Soc.* 162 (2015) D275–D282.
- [57] G. Tabbi, A. Giuffrida, R.P. Bonomo, *J. Inorg. Biochem.* 128 (2013) 137–145.
- [58] H. Masuda, T. Sugimori, A. Odani, O. Yamauchi, *Inorg. Chim. Acta* 180 (1991) 73–79.